Gas Sensor Array Based on Metal-Decorated Carbon Nanotubes

Alexander Star,* Vikram Joshi, Sergei Skarupo, David Thomas, and Jean-Christophe P. Gabriel†

Nanomix Inc., Emeryville, California 94608

Received: July 11, 2006; In Final Form: August 21, 2006

Here we demonstrate design, fabrication, and testing of electronic sensor array based on single-walled carbon nanotubes (SWNTs). Multiple sensor elements consisting of isolated networks of SWNTs were integrated into Si chips by chemical vapor deposition (CVD) and photolithography processes. For chemical selectivity, SWNTs were decorated with metal nanoparticles. The differences in catalytic activity of 18 catalytic metals for detection of H_2, CH_4, CO, and H_2S gases were observed. Furthermore, a sensor array was fabricated by site-selective electroplating of Pd, Pt, Rh, and Au metals on isolated SWNT networks located on a single chip. The resulting electronic sensor array, which was comprised of several functional SWNT network sensors, was exposed to a randomized series of toxic/combustible gases. Electronic responses of all sensor elements were recorded and the sensor array data was analyzed using pattern-recognition analysis tools. Applications of these small-size, low-power, electronic sensor arrays are in the detection and identification of toxic/combustible gases for personal safety and air pollution monitoring.

Introduction

Sensor arrays, which are often called electronic noses, mimic nature by combining artificial computational capability and pattern-recognition based sensing architectures.[1] A sensor array achieves selectivity by providing a characteristic signature for an analyte derived from the global response of the sensors contained within the array. To date, sensor modalities include surface acoustic wave and bulk resonating quartz crystal devices, micromachined cantilevers, conducting polymers, semiconducting metal oxide resistors, chemically sensitive field-effect transistors (FETs), and carbon-black−polymer composites.[2] Miniaturization of sensor elements is important for the design of high-density sensor arrays with relatively small spatial footprints. Recently, electronic devices utilizing active elements made of nanowires[3] and carbon nanotubes[4−10] have been shown to function as extremely sensitive and small chemical sensors. Integration of these sensor elements into a complex sensor array may bring about electronic noses as complex as the mammalian olfactory system.[11]

The basic concept of chemical gas detection using a carbon nanotube field-effect transistor (NTFET) is illustrated in Figure 1A. Single-walled carbon nanotubes (SWNTs) integrated into a Si platform have a characteristic electrical conductance that can be measured by applying a voltage. As an analyte comes into contact with the SWNT, network conductance is modified to produce a detection signal. Specific sensitivity of NTFET sensors can be achieved by employing recognition layers, which induce chemical reactions that modify the NTFET device characteristics. This sensing design recently has been demonstrated for detection of various chemical and biological analytes.[6−10,12] In particular, a catalytic metal (Pd) was used to decorate SWNTs toward detection of H_2 and CH_4 at ambient temperatures.[6,8]

Thermal and electron-beam evaporation previously have been used for metal deposition on sidewalls of SWNTs.[13] Electrochemical deposition, compared to other methods, offers significantly higher control over the purity and the amount of material deposited onto the nanotube surface.[14] To date, several procedures have been published[15] for the electrodeposition of noble metals on SWNTs under direct potential control. Choi et al. has reported[16] spontaneous metal deposition on SWNT sidewalls, creating a simple and elegant technique to produce metal-decorated carbon nanotubes. However, this method could not allow any site-specific metal deposition on a device chip, and precise deposition of metal species at specific locations is a requirement for the fabrication of a sensor array. Site-specific metal deposition can be accomplished using electrochemical galvanic displacement[17,18] by (1) connecting a specific nanotube device to a metal substrate having a red./ox. potential far lower than the metal to be deposited, and (2) immersing the device into a solution of the metal cation to be reduced and deposited. This closes the circuit of an electrochemical cell and induces metal deposition on nanotube surfaces upon application of an appropriate potenitial. Through the use of this method, selected NTFET devices can be decorated with metal nanoparticles of different catalytic metals (Au, Pt, Pd, Rh, etc.) while leaving other devices unmodified on a single chip.

In our study, we expanded evaporation and electrodeposition approaches for detection of important toxic/combustible gases by using a sensor array approach. We elucidated the nature of NTFET sensing by comparing the performance of different catalytic metals and demonstrated a sensor array based on cross-sensitive NTFET sensor elements decorated with different catalytic metals. In addition, we compare the sensitivity of metal-decorated nanotubes produced by evaporative and electrochemical methods and discuss the applicability of both as components in nanoscale sensor arrays.

† This article is dedicated to the memory of Dr. Lucy M. Bull, loving wife of Jean-Christophe P. Gabriel.

* To whom correspondence should be sent at the present address: Department of Chemistry, University of Pittsburgh. E-mail: astar@pitt.edu.

10.1021/jp064371z CCC: $33.50
Published on Web 10/04/2006

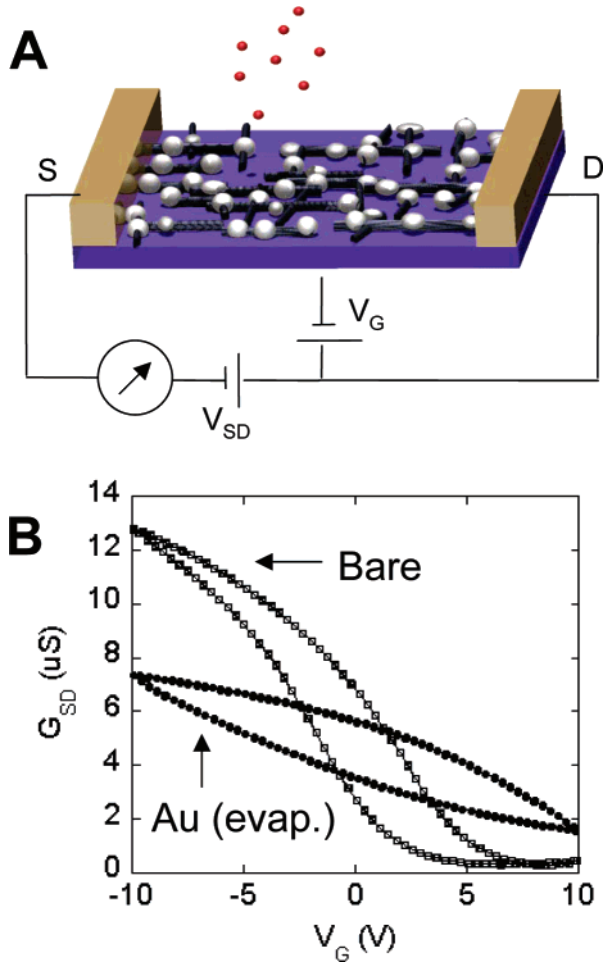

Figure 1. (A) Conceptual illustration of a carbon nanotube network connecting source (S) and drain (D) electrodes of a FET. SWNTs are decorated with metal nanoparticles (silver bullets) for selective detection of analyte gases (red dots). (B) Electronic measurements, such as source-drain conductance (G_{SD}), as a function of gate voltage (V_g) before (bare) and after thermal evaporation of discontinuous layer of gold (Au evap).

Experimental Section

Carbon Nanotube Devices. NTFET devices were fabricated using SWNTs grown via chemical vapor deposition (CVD) at 900 °C using dispersed iron nanoparticles as a growth promoter and a methane/hydrogen gas mixture on doped Si 100 mm wafers with SiO_2 at its surface as was reported previously.[10,12] Electrical leads were patterned on top of the nanotubes from 30-nm-thick Ti films capped with a 120-nm-thick Au layer using standard photolithography techniques. Each wafer consists of about one thousand dies with 2.54 × 2.54 mm^2 dimensions. On each die, a random network of SWNTs is patterned into several devices that consist of two parallel electrodes. SWNTs outside the device areas were removed by using oxygen plasma to electrically isolate each device. Scanning electron microscopy (SEM) (Leo) and atomic force microscopy (AFM) (Digital Instruments) were used for process quality assurance; NTFET electronic characteristics were collected using an autoprobe tester. Transfer characteristics (i.e., source-drain conductance vs gate voltage, $G-V_g$) were measured in air with the gate voltage applied to the doped Si substrate and were consistent with *p*-type, positive threshold voltages, as described elsewhere.[19]

Metal Deposition. NTFET devices were decorated by thermal and electron-beam evaporation of Mg, Al, Ti, V, Cr, Mn, Fe, Co, Ni, Zn, Mo, Rh, Pd, Sn, W, Pt, Au, and Pb metals.[20] In this approach, all NTFET devices on the Si chip were decorated with noncontinuous films of one metal/metal oxide. Evaporation was performed using Edward Auto 306 e-beam evaporator. Metal targets were purchased from Aldrich.

Metal electrodeposition was accomplished by electrically grounding a specific NTFET device on the Si chip (Supporting Information, Figure S1A). The Si chip with multiple NTFET devices was placed on an aluminum block with this block being electrically grounded. Metal pins were pushed onto two of the Ti/Au contacts that were related to a single NTFET device, thus making electrical contact. These metal pins were electrically grounded. The chip was rinsed with a 1:1 mixture of H_2O and EtOH for cleaning. A 5 mM solution of $PdCl_2$ in a 1:1 mixture of H_2O and EtOH was prepared. Five drops of the solution were placed on the substrate with the solution contacting both the substrate and the underlying Al block. After 30 s, the solution was rinsed off with a 1:1 mixture of H_2O and EtOH, and the Si chip was dried with a stream of compressed air.

Transmission Electron Microscopy (TEM). The preparation of metal-decorated SWNTs for TEM was carried out as follows: The CVD grown SWNTs were removed from the surface of a 100-mm silicon wafer by ultrasonication of several small pieces in 1,2-dichlorobenzene for 5 min. Drops of the nanotube suspension were deposited onto a lacey carbon film 300 mesh copper TEM grid, resulting in individual tubes on the surface. The standard electrodeposition procedure was applied by electrically grounding the TEM grid while on an Al substrate. A 5 mM $PdCl_2$ solution (H_2O/EtOH) was deposited to cover both the TEM grid and the substrate.

Electronic Measurements. The NTFET custom test fixture measures an array of up to 12 separate sensors and controls gas delivery as well (Supporting Information, Figure S1B,C). The housing consists of a modified shielded I/O board (SCB-68, National Instruments) with a 40-pin zero insertion force (ZIF) socket and mounting screws for a gas delivery manifold. The I/O board was linked to a PC, and a data acquisition card (PCI-6014, National Instruments) controlled the board. Programming to manage data acquisition and control gas exposure for the system was performed by us in LabVIEW (National Instruments). An analogue output voltage was used to sweep the gate of the NTFETs. A gas diluter (Precision Gas Diluter, model 1010, Custom Sensor Solutions) delivered the desired concentrations of selected gases to the manifold. Device characteristics such as source-drain voltage and current were calculated in LabVIEW from voltage measurements across precision sense resistors.

Results and Discussion

Evaporative Metal Deposition. We first consider the sensor response of NTFET devices decorated with Mg, Al, Ti, V, Cr, Mn, Fe, Co, Ni, Zn, Mo, Rh, Pd, Sn, W, Pt, Au, and Pb metals via thermal or electron-beam evaporation.[20] In this approach, metal deposition is not specific, and all NTFET devices on the chip were decorated with the same metal/metal oxide. After metal decoration, all devices demonstrated a conductance that was less sensitive to gate voltages, as indicated in Figure 1B. Nonspecific metal deposition resulted in device conductance corresponding to neither "on" or "off" values of the undecorated devices, and in general, were found to approximately equal the zero gate voltage conductance. We have found that thickness of the deposited metal layer has a significant effect on the device characteristics. Increasing metal thickness results in a decrease of the device modulation (sensitivity to gate voltages) followed by an electrical shorting of the devices. Metal deposition on

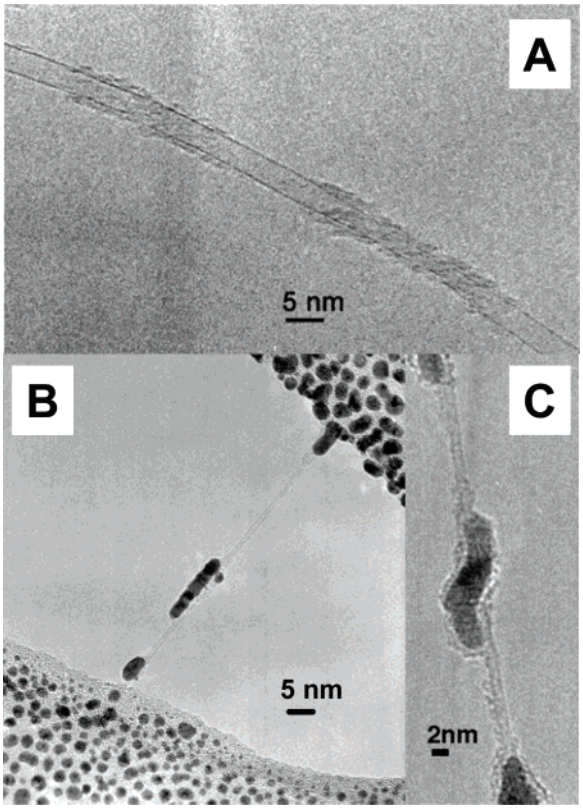

Figure 2. (A) HRTEM image of CVD-grown SWNTs deposited onto a lacey carbon film 300 mesh copper TEM grid prior metal decoration. (B) HRTEM image of an individual SWNT bridging across TEM support film after e-beam evaporation of palladium. While nanoparticles are equally distributed on a grid, they tend to clump together on sidewalls of SWNT. (C) Close-up of metal nanoparticles decorating a SWNT.

control devices with no SWNTs between source and drain electrodes showed zero conductivity as long as the noncontinuous metal layer was deposited. Therefore, we believe that the electrical conduction passes through the nanotube network, rather than through the noncontinuous metal layer. The observed loss of gate dependence after metal evaporation (Figure 1B) can be attributed to screening induced by metal nanoparticles.[21]

To characterize the metal layers on SWNTs, we employed high-resolution transmission electron microscopy (HRTEM). For HRTEM studies, SWNTs were removed from the surface of devices by sonication and deposited on TEM grids. TEM grids with SWNTs were placed in the metal evaporator alongside Si chips containing the NTFET devices. HRTEM images of SWNTs before and after metal evaporation are presented in Figure 2. Metal deposition on sidewalls of SWNTs yields isolated metal islands, and discontinuous metal layers are observed on the TEM grid as well. HRTEM images reveal the presence of amorphous carbon on sidewalls of the SWNT, which originated from CVD growth. Interestingly, metal deposition is primarily observed on areas of SWNT sidewalls covered with the amorphous carbon. In addition to improving metal adhesion to SWNT sidewalls, amorphous carbon is not expected to affect the gas response of the NTFET devices because of averaging effects of the random network device geometry.

After metal evaporation, the Si chips with NTFET devices were packaged and tested with four combustible gases: H_2, CH_4, CO, and H_2S. The gas testing was done in air at room temperature at constant relative humidity. Gases were introduced at two concentrations for 18 min each as presented in Figure 3 (response of selected NTFET devices to binary gas mixtures is presented in Supporting Information, Figure S2 and Table S1). Although additional information can be collected by measuring

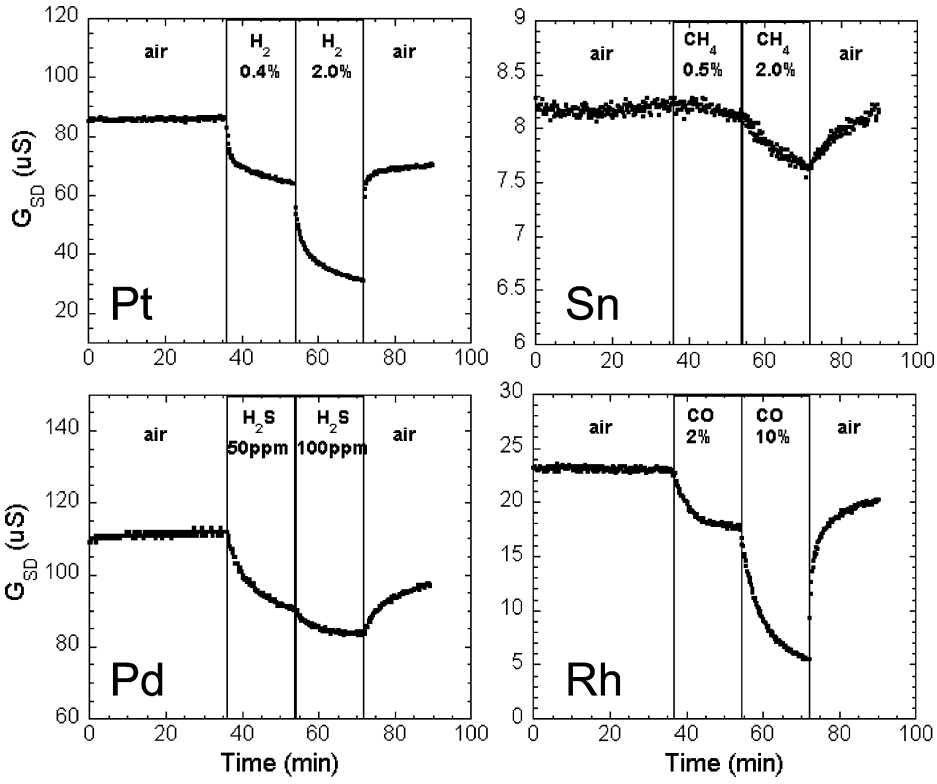

Figure 3. Response of carbon nanotube sensors functionalized with different catalytic metals (Pt) for H_2 (0.4 and 2% in air), (Sn(SnO_2)) for CH_4 (0.5 and 2% in air), (Pd) for H_2S (50 and 100 ppm in air), and (Rh) for CO (2 and 10% in air) at room temperature. NTFET conductance was measured at $V_g = 0$.

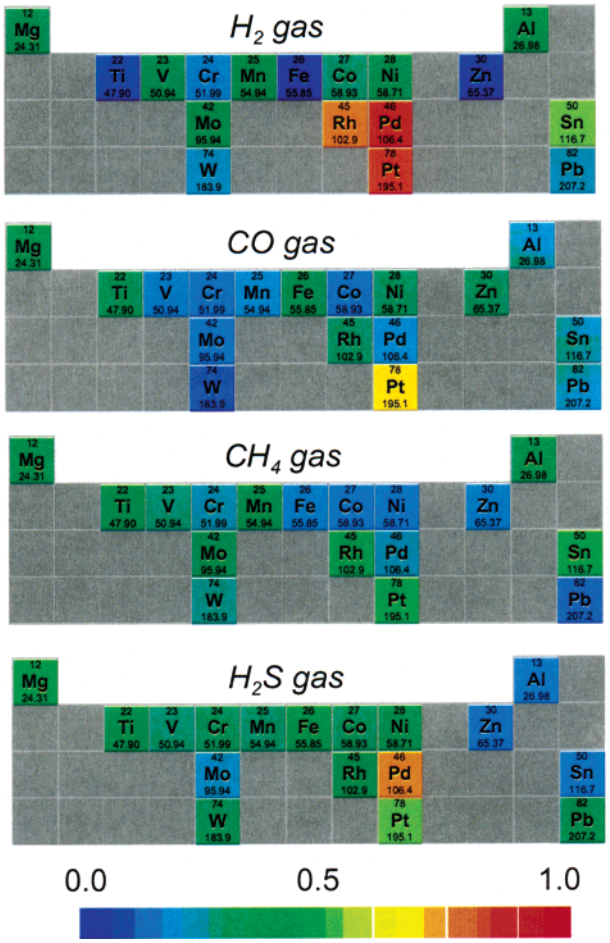

Figure 4. Correlation coefficients relating the conductance of devices decorated via metal evaporation with the gas profile of the tested gases, from 0 (no response) to 1 (maximal response). The catalytic metals were evaporated on carbon nanotube devices and tested for H_2, CO, CH_4, and H_2S gases as highlighted in the Periodic Table.

$G-V_g$ characteristics (vide infra), in these experiments only device conductivity at zero gate voltage was measured as a function of the device exposure to the combustible gases.

The electronic response of metal-decorated NTFET devices to all four combustible gases was similar in that the presence of a combustible gas resulted in a decrease in the device conductance. However, we have found that both the magnitude of response and the response time differed for each tested gas/metal combination. This observation implies that a combination of metals is required to achieve specificity for a particular gas analyte. To quantify the sensor response, we have applied Pearson's product moment correlation to the device conductance and the tested gas profile.[22] The calculated correlation coefficients quantify how well a certain gas was detected at the tested conditions. Their values were plotted as color gradients on a periodic table (Figure 4) for each gas. Although individual metals are cross-sensitive to the tested gases, the resulting color spectrum shows a distinguishable pattern for each gas, meaning analyte specificity can be achieved by recognizing patterns produced from the response of a sensor array consisting of multiple NTFET devices with each functionalized with a different catalytic metal.

Electrochemical Metal Deposition. For sensor array fabrication, the electrodeposition process was performed for multiple NTFET devices on a single Si chip. Pd, Rh, Pt, and Au were selected for electrodeposition because of the catalytic properties

TABLE 1: Sensor Array Test Conditions[a]

test gas	*p*, ppm
CO	2500
H_2	10000
H_2S	50
NH_3	200
NO_2	5

[a] Test sequence: CO, H_2, NH_3, H_2, H_2S, NO_2, NO_2, NO_2, H_2, H_2, NO_2, H_2S, NH_3, NH_3, H_2, H_2S, H_2S, CO, NO_2, CO, H_2S, NH_3, CO, NH_3, CO.

that were demonstrated in the evaporative technique. The following 5 mM metal salt solutions, $PdCl_2$, Na_3RhCl_6, Na_2PtCl_4, and $HAuCl_4$, were used in a 1:1 mixture of H_2O and EtOH to deposit NTFET devices with Pd, Rh, Pt, and Au, respectively. With this method, different NTFET devices on the same chip were decorated with four different catalytic metal nanoparticles (two NTFET devices for each metal), while leaving other devices unmodified (Figure 5A,B). We successfully have deposited the metals on different devices in different orders with no cross deposition between metals. The content of nanoparticles on a single device was confirmed by elemental analysis to be of only a single metal.

We have used microscopy to characterize metal-decorated SWNTs produced by the electroplating procedure. As evident from scanning electron microscopy (SEM) studies (Figure 5C), metal nanoparticles coating is not uniform: Although metal evaporation results in the uniform distribution of metal nanoparticles on the device surface,[13] the electroplating process produces metal nanoparticles only on the sidewalls of SWNTs. The electroplating process results after 60 s in significantly larger metal coverage of SWNTs as compared to metal evaporation technique (Figure 2) with a mean particle size of $\sim$ 200 nm, although it has been shown that excellent control over metal deposition can be maintained by controlling deposition time and cell potential.[23] HRTEM studies reveal that these large metal nanoparticles consist of multiple metal clusters of 3−5 nm (Figure 5D). This observation suggests that the electroplating process happens in multiple stages.

Sensor Array Gas Testing. Electroplated devices were tested for three combustible gases, H_2, CO, and H_2S (since methane has not demonstrated any significant response at room temperature), and two toxic gases, NH_3 and NO_2. The NTFET response to a single gas exposure was recorded as change in conductance (G) versus gate voltage (V_g) (Figure 6; Supporting Information has four animations of $G-V_g$ changes during the gas exposure). The effect of NH_3 and NO_2 on devices including bare devices (no electroplating) was a shift in device characteristics similarly to what was reported in the literature.[4] Exposure to NH_3 gas produced a shift to more negative gate voltage and a decrease in conductance, while adsorption of NO_2 gas on NTFET devices resulted in an opposite shift to a more positive gate voltage and a general increase in device conductance (Figure 6A,B). This response to NH_3 and NO_2 has been discussed in depth in the literature[4,10,24] and is attributed to either SWNT channel doping with electrons and holes for NH_3 and NO_2, respectively, or effective changes in the Schottky barrier. Interestingly, the observed sensor response of metal-decorated NTFET devices to exposures of H_2 and H_2S gases at room temperature (Figure 6C,D) was quite different. Metal-decorated devices demonstrated a decrease in conductance without any apparent shift in the $G-V_g$ characteristics. The observed differences have certain ramifications on the underlying sensor mechanism.

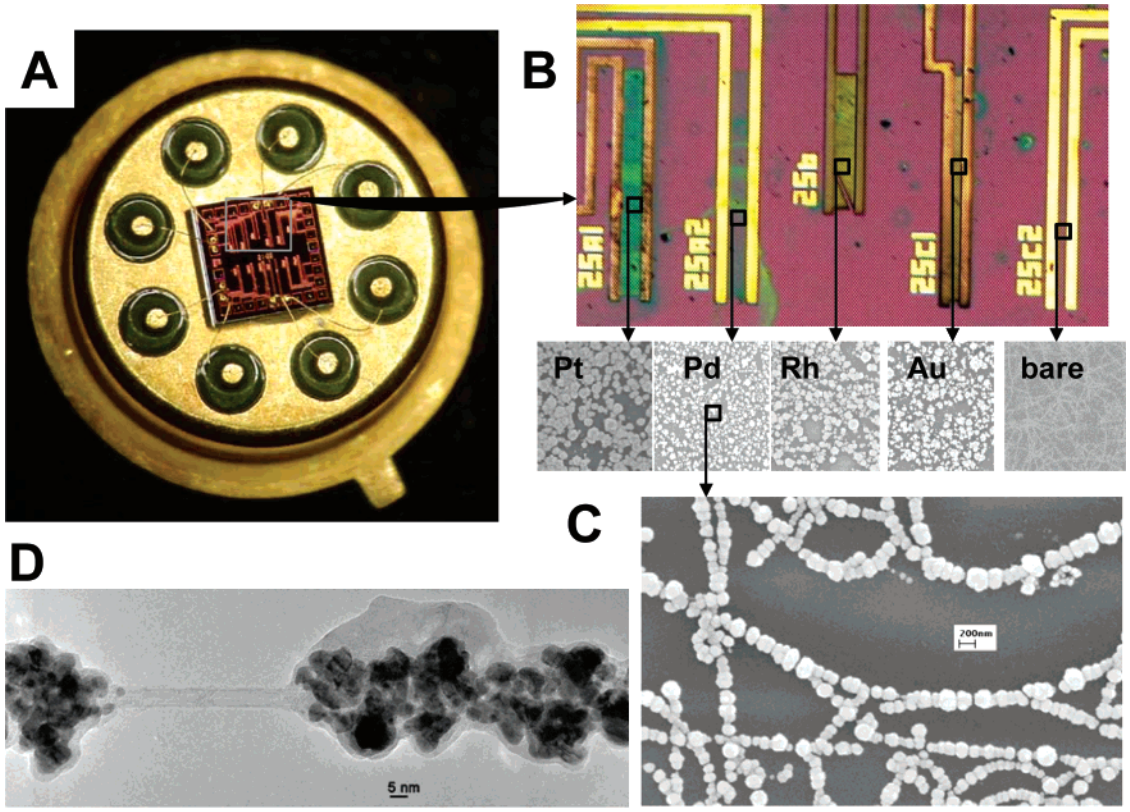

Figure 5. (A) Si chip (2 mm × 2 mm) containing multiple carbon nanotube network devices. (B) Optical microscope photograph (200X) of five pairs of metal electrodes connecting isolated networks of nanotubes after individual electroplating with metals on four pairs. No metal was deposited to the fifth pair of electrodes. (C) Scanning electron microscopy (SEM) images of the nanotube networks between the electrode pairs after metal electroplating (Scale bar is 200 nm). (D) HRTEM image of Pd nanoparticles electroplated on SWNTs. (Scale bar is 5 nm). Nanotubes were deposited on a TEM grid prior to electroplating step.

TABLE 2: PLS Multiple Correlation Coefficients (R^2) and *p*-values

test gas	R^2	*p*-value
CO	0.142	0.675
H_2	0.909	0.000
H_2S	0.842	0.000
NH_3	0.769	0.000
NO_2	0.684	0.000

The nanoelectronic sensor array was exposed to CO, H_2, H_2S, NH_3, and NO_2 gases with five exposures to each gas (Table 1). The order of exposure was randomized[25] to separate the desired signal from the possible effects of drift and poisoning of the sensors and any uncontrolled changes in the gas delivery system. Responses of nine NTFET devices (channels) to a sequence of 25 gas exposures (measured as device conductance at zero gate voltage) are presented in Supporting Information, Figure S3. A single gas exposure consisted of a 5-minute settling period and a 5-minute exposure to gas followed by a 10-minute recovery period. Selected animations of the full $G-V_g$ curves recorded during single gas exposures and the derived conductance are presented in Supporting Information.

Sensor Array Data Analysis. For sensor array data analysis, we employed the classical methods of principal component analysis (PCA) and partial least squares regression (PLS Regression), which provide an efficient approach for reducing the dimensionality of a data set.[2] The analysis was performed with the aid of MINITAB statistical software. To simplify data processing, we have examined the conductance at zero gate voltage. For data analysis purposes, the mean over the first 100 s of the test was used to represent the response to air, and the mean over the last 100 s of gas exposure was the response to the test gas in a given test. A more detailed explanation of the statistical methods used and PCA results are available in Supporting Information.

A multivariate PLS regression model makes it possible not only to see whether the system has a distinct response to each analyte but also to calculate the magnitude of the response in original units.[26] Here we use the term multivariate to imply multiple predictors and multiple responses. Listed in Table 2 are the PLS multiple correlation coefficients (R^2), which we use as a simple goodness-of-fit measure, and their corresponding *p*-values, which indicate the probability of randomly obtaining the same or better fit. The values for CO indicate that we did not obtain a good fit for that analyte, indicating a lack of sensor array sensitivity toward this gas. We used the resulting model to calculate the sensor array output signal for four analytes in this experiment (Figure 7). Although individual NTFET channels are cross-sensitive to multiple gases (Supporting Information, Figure S3), the PLS output demonstrates selective responses of the sensor array for four gases from the sequence of 25 gas exposures.

Devices fabricated via electrodeposition show similar selectivity as those fabricated by metal evaporation with one distinct advantage: a much smaller size. Nonlithographic evaporative methods lack the capability to selectively deposit metal at a specific site, resulting in an entire device chip to be decorated with the same metal. On the other hand, electrodeposition shows great promise for a sensor array fabrication. The ability to deposit many different metals on a single chip allows two design benefits: (1) reduction of device size and (2) an increased number of analyte specific locations compared to traditional devices. By reducing the size of each analyte specific sensor component, more components, and therefore a greater breadth

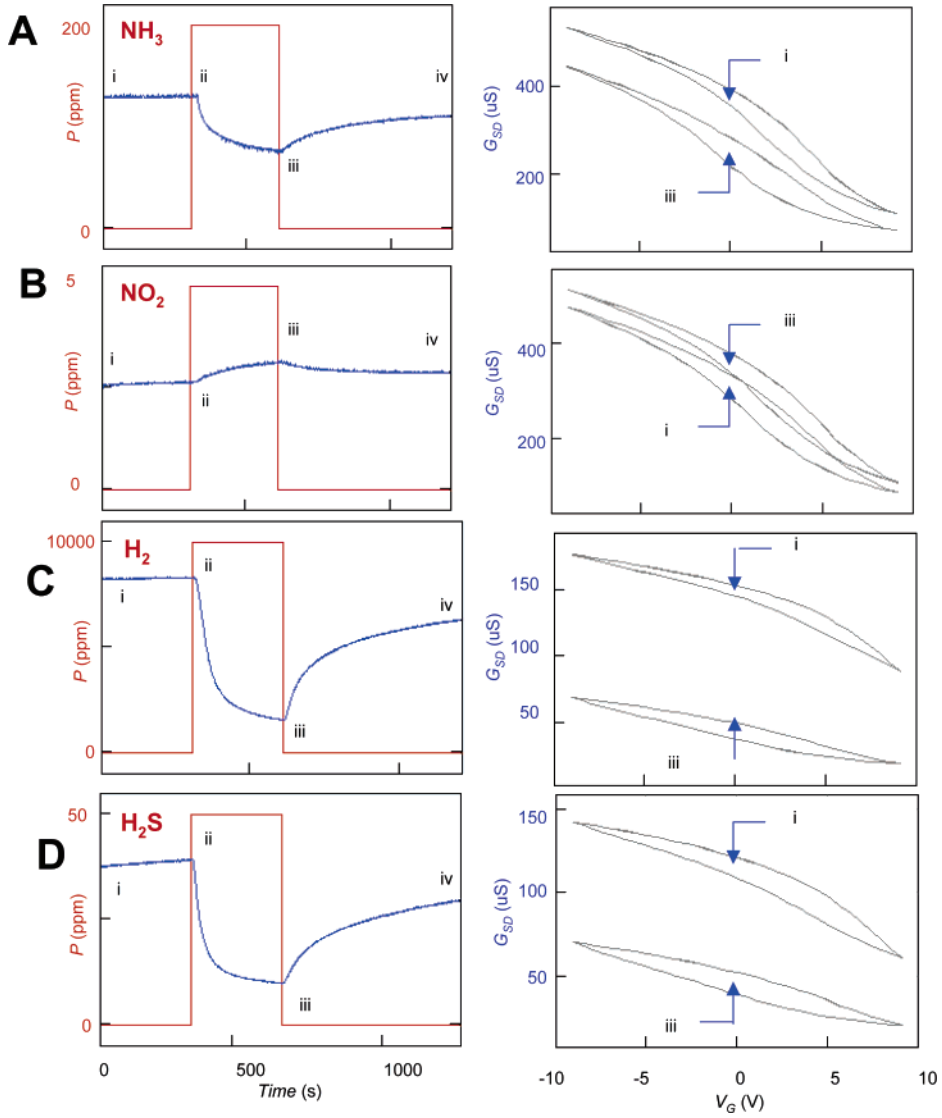

Figure 6. Response of bare NTFET device to (A) NH_3 and (B) NO_2 gases; response of Pd-decorated NTFET device to (C) H_2 and (D) H_2S gas. Left: A single gas exposure (red line) consisted of (i−ii) a five-minute settling period, (ii−iii) five-minute exposure to gas followed by (iii−iv) a ten-minute recovery period. NTFET conductance (G at $V_g = 0$, blue curve) is derived from the $G-V_g$ curves measured during the test. Right: $G-V_g$ curves recorded before and after gas introduction. Animations showing $G-V_g$ curves recorded during single gas exposures and the derived conductance are available as AVI files in Supporting Information.

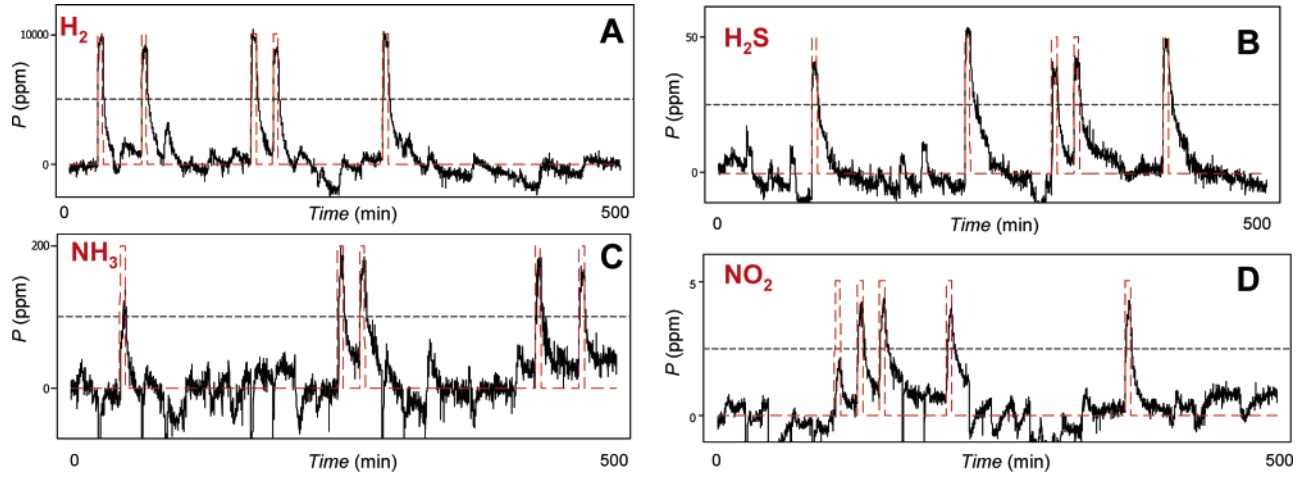

Figure 7. PLS regression of the sensor array. Sensor array response to (A) H_2 gas, (B) H_2S gas, (C) NH_3 gas, and (D) NO_2 gas. Dashed red: test gas concentration. Solid black: calibrated output of sensor array. Dashed black: possible detection thresholds.

of analysis, can be incorporated into a smaller sensor array. This will provide greater sensor performance with a less invasive footprint, and in application, the capabilities of this technique only would be limited by the number of devices on a chip.

Conclusion

In conclusion, we have fabricated a nanoelectronic sensor array that consists of NTFETs with networks of SWNTs as conducting channels. We have compared the responses of devices decorated via site-specific electrodeposition to conventional metal evaporation process. In both cases, NTFETs were found to be decorated with nanoparticles of catalytic metals and demonstrated chemical selectivity and were capable of working as a sensor array. The sensor arrays were tested electronically with five toxic/flammable gases, and the output of the sensor array was analyzed using the PLS regression method to yield recognition of the gases. The array chip fabricated via electrodeposition and containing multiple functionalized NTFET devices demonstrates comparative selectivity to traditional metal evaporation techniques but has a much smaller spatial footprint. Employment of metal/metal oxide nanoparticles as gas recognition layers makes the carbon nanotube sensor arrays more robust and suitable to real life applications. Applications for these small-size, low-power nanoelectronic sensor arrays are in detection and identification of toxic/explosive gases for personal safety and air pollution monitoring.

Acknowledgment. The authors wish to thank Dr. M. V. P. Altoé (Lawrence Berkeley National Laboratory, LBNL) for conducting the HRTEM measurements. The research at Nanomix was partially supported by the U.S. Environmental Protection Agency. We thank the technical staff at Nanomix for their assistance with device fabrication and measurements. We are indebted to the National Center for Electron Microscopy at the LBNL for making this facility available to us.

Supporting Information Available: NTFET sensor array test fixture; H_2 cross-sensitivity experiments; four $G-V_g$ animations of sensor array responses to various gas exposures. This material is available free of charge via the Internet at http://pubs.acs.org

References and Notes

(1) Gardner, J. W.; Barlett, P. N. *Electronic Noses: Principles and Applications*; Oxford University Press: Oxford, U.K., 1999.

(2) Albert, K. J.; Lewis, N. S.; Schauer, C. L.; Sotzing, G. A.; Stitzel, S. E.; Vaid, T. P.; Walt, D. R. *Chem. Rev.* **2000**, *100*, 2595−2626. Jurs, P. C.; Bakken, G. A.; McClelland, H. E. *Chem. Rev.* **2000**, *100*, 2649−2678. Stetter, J. R.; Penrose, W. R. *Understanding Chemical Sensors and Chemical Sensor Arrays (Electronic Noses): Past, Present, and Future*; Wiley-VCH: Weinheim, Germany, 2002; Chapter 2.3 in Sensor Update, Vol. 10, pp 189−229. Lewis, N. S. *Acc. Chem. Res.* **2004**, *37*, 663−672.

(3) Cui, Y.; Wei, Q. Q.; Park, H. K.; Lieber, C. M. *Science* **2001**, *293*, 1289−1292. Favier, F.; Walter, E. C.; Zach, M. P.; Benter, T.; Penner, R. M. *Science* **2001**, *293*, 2227−2231. Kolmakov, A.; Zhang, Y.; Cheng, G.; Moskovits, M. *Adv. Mater.* **2003**, *15*, 997−1000.

(4) Kong, J.; Franklin, N. R.; Zhou, C.; Chapline, M. G.; Peng, S.; Cho, K.; Dai, H. *Science* **2000**, *287*, 622−625.

(5) Collins, P. G.; Bradley, K.; Ishigami, M.; Zettl, A. *Science* **2000**, *287*, 1801−1804.

(6) Kong, J.; Chapline, M. G.; Dai, H. *Adv. Mater.* **2001**, *13*, 1384−1386.

(7) For a sensor array comprising two polymer coated NTFET devices, see: Qi, P.; Vermesh, O.; Grecu, M.; Javey, A.; Wang, O.; Dai, H. J.; Peng, S.; Cho, K. J. *Nano Lett.* **2003**, *3*, 347−351.

(8) Lu, Y.; Li, J.; Han, J.; Ng, H.-T.; Binder, C.; Partridge, C.; Meyyappan, M. *Chem. Phys. Lett.* **2004**, *391*, 344−348.

(9) Novak, J. P.; Snow, E. S.; Houser, E. J.; Park, D.; Stepnowski, J. L.; McGill, R. A. *Appl. Phys. Lett.* **2003**, *83*, 4026−4028. Staii, C.; Johnson, A. T.; Chen, M.; Gelperin, A. *Nano Lett.* **2005**, *5*, 1774−1778.

(10) Bradley, K.; Gabriel, J.-C. P.; Briman, M.; Star, A.; Grüner, G. *Phys. Rev. Lett.* **2003**, *91*, 218301. Bradley, K.; Gabriel, J.-C. P.; Grüner, G. *Nano Lett.* **2003**, *3*, 1353−1355. Star, A.; Han, T.-R.; Joshi, V.; Gabriel, J.-C. P.; Grüner, G. *Adv. Mater.* **2004**, *16*, 2049−2052.

(11) Mombaerts, P. *Science* **1999**, *286*, 707−711. Mori, K.; Nagao, H.; Yoshihara, Y. *Science* **1999**, *286*, 711−715. Sobel, N.; Khan, R. M.; Saltman, A.; Sullivan, E. V.; Gabrieli, J. D. E. *Nature* **1999**, *402*, 35.

(12) Star, A.; Gabriel, J.-C. P.; Bradley, K.; Grüner, G. *Nano Lett.* **2003**, *3*, 459−463. Chen, R. J.; Bangsaruntip, S.; Drouvalakis, K. A.; Wong Shi Kam, N.; Shim, M.; Li, Y.; Kim, W.; Utz, P. J.; Dai, H. *Proc. Natl. Acad. Sci. U.S.A.* **2003**, *100*, 4984−4989. Besteman, K.; Lee, J.-O.; Wiertz, F. G. M.; Heering, H. A.; Dekker, C. *Nano Lett.* **2003**, *3*, 727−730. Boussaad, S.; Tao, N. J.; Zhang, R.; Hopson, T.; Nagahara, L. A. *Chem. Commun.* **2003**, 1502−1503. Chen, R. J.; Choi, H. C.; Bangsaruntip, S.; Yenilmez, E.; Tang, X.; Wang, Q.; Chang, Y.-L.; Dai, H. *J. Am. Chem. Soc.* **2004**, *126*, 1563−1568. Star, A.; Tu, E.; Niemann, J.; Gabriel, J.-C. P.; Joiner, C. S.; Valcke, C. *Proc. Natl. Acad. Sci. U.S.A.* **2006**, *103*, 921−926.

(13) Zhang, Y.; Dai, H. *Appl. Phys. Lett.* **2000**, *77*, 3015−3017. Zhang, Y.; Franklin, N. W.; Chen, R. J.; Dai, H. *Chem. Phys. Lett.* **2000**, *331*, 35−41.

(14) Batail, P.; Boubekeur, K.; Fourmigué, M.; Gabriel, J.-C. P. *Chem. Mater.* **1998**, *10*, 3005−3015.

(15) Quinn, B. M.; Dekker: C.; Lemay, S. G. *J. Am. Chem. Soc.* **2005**, *127*, 6146−6147. Day, T. M.; Unwin, P. R.; Wilson, N. R.; Macpherson, J. V. *J. Am. Chem. Soc.* **2005**, *127*, 10639−10647.

(16) Choi, H. C.; Shim, M.; Bangsaruntip, S.; Dai, H. *J. Am. Chem. Soc.* **2002**, *124*, 9058−9059.

(17) Okinaka, Y.; Hoshino, M. *Gold Bull.* **1998**, *31*, 3−13. Porter, L. A.; Choi, H. C.; Ribbe, A. E.; Buriak, J. M. *Nano Lett.* **2002**, *2*, 1067−1071.

(18) Qu, L.; Dai, L. *J. Am. Chem. Soc.* **2005**, *127*, 10806−10807.

(19) Although approximately one-third of as-deposited SWNTs are metallic, NTFET channel length and density of the nanotube network can be optimized below percolation threshold for metallic SWNTs, thus providing NTFET devices with high on−off ratio. Gabriel, J.-C. P. *Mater. Res. Soc. Symp. Proc.* **2003**, *776*, Q12.7.1. Snow, E. S.; Novak, J. P.; Campbell, P. M.; Park, D. *Appl. Phys. Lett.* **2003**, *82*, 2145−2147. Alam, M. A.; Pimparkar, N.; Kumar, S.; Murthy, J. *MRS Bull.* **2006**, *31*, 466−470.

(20) Except for noble metals, the deposited metal nanoparticles are partially or fully oxidized at ambient conditions.

(21) Kim, B.-K.; Park, N.; Na, P. S.; So, H.-M.; Kim, J.-J.; Kong, K.-J.; Chang, H.; Ryu, B.-H.; Choi, Y.; Lee, J.-O. *Nanotechnology* **2006**, *17*, 496−500.

(22) Dunham, M. H. *Data Mining, Introductory and Advanced Topics*; Prentice Hall: New York, 2003.

(23) Fan, Y.; Goldsmith, B. R.; Collins, P. G. *Nat. Mater.* **2005**, *4*, 906−911. Cui, H. F.; Ye, J. S.; Zhang, W. D.; Wang, J.; Sheu, F. S. *J. Electroanal. Chem.* **2005**, *577*, 295−302.

(24) Lee, C. Y.; Strano, M. S. *Langmuir* **2005**, *21*, 5192−5196. Zhang, J.; Boyd, A.; Tselev, A.; Paranjape, M.; Barbara, P. *Appl. Phys. Lett.* **2006**, *88*, 123112.

(25) Wu, J.; Hamada, M. *Experiments: Planning, Analysis, and Parameter Design Optimization*; Wiley: New York, 2000.

(26) Geladi, P.; Kowalski, B. R. *Anal. Chim. Acta* **1986**, *185*, 1−17.